[Article] DOI: 10.13208/j.electrochem.2214005 Http://electrochem.xmu.edu.cn

A Self-Supported Ru-Cu_3P Catalyst toward Alkaline Hydrogen Evolution

Zi-Xuan Wan[#], Chao-Hui Wang[#], Xiong-Wu Kang[*]
(*New Energy Research Institute, School of Environment and Energy, South China University of Technology, Higher Education Mega Center, Guangzhou 510006, Guangdong, China*)

Abstract: Transition metal phosphide (TMP) is a kind of effective catalysts toward hydrogen evolution reaction (HER) in alkaline electrolytes. However, the performance of TMP catalysts is strongly limited by water splitting. In this work, we developed a method to prepare a copper foam (CF) supported Ru-doped Cu_3P catalyst (Ru-Cu_3P/CF) by a consecutive growth of $Cu(OH)_2$ nanoarrays, soaking in $RuCl_3$ solution and phosphorization. A large surface area was obtained by the self-supported catalysts with the appropriative Ru doping. As an excellent HER catalyst, it exhibited a low overpotential of 95.6 mV at a current density of 10 mA·cm^{-2}, which is 149.4 mV lower than that of Cu_3P/CF without Ru-doping. The Tafel slope was reduced from 136.6 to 73.6 mA·dec^{-1} and the rate determining step was changed from Volmer step to Heyrovsky step. The improvement of HER performance might be attributed to the facilitated water splitting step by Ru-doping, which provides more active sites for water splitting. The nanoparticles morphology of Ru-Cu_3P derived from the $Cu(OH)_2$ arrays ensured large electrochemical surface areas of the supported electrodes, which could promote the mass and electron transfers, and promote gas production and bubble release. This work highlights the importance of the tuning of the water splitting step and surface engineering by the transition metal with emptier d orbitals, which may pave the road for design of high-performance HER electrocatalyst.

Key words: electrocatalysis; water splitting; hydrogen evolution; copper phosphide; Ru-doping

1 Introduction

It is imminent to develop renewable energy to alleviate environmental problems caused by consumption of traditional fossil fuels[1]. Due to the high energy density and environmental friendliness, hydrogen energy is considered as a potential green energy. Renewable energy-driven electrolytic water splitting[2], which is recognized as a hydrogen production technology with broad market prospects and application potential, is expected to build a clean and sustainable carbon-free energy system in future[3]. In an actual electrolyzer, hydrogen evolution reaction (HER) on a cathode requires a high overpotential to maintain high production rates of hydrogen[4], which reduces the energy conversion efficiency and increases the cost of hydrogen production[5]. In order to reduce reaction overpotential and energy consumption, HER usually requires active electrocatalysts[6]. So far, platinum-based materials have been the benchmark of the catalytic electrocatalysts[7]. However, their large-scale use is limited by the high cost and scarcity on earth. Therefore, it is urgent to develop low-cost, high-efficiency and stable HER electrocatalysts[8].

Over the past few decades, a series of HER catalysts with high catalytic activity have been explored[9], which leads to the development of several novel tran-

Cite as: Wan Z X, Wang C H, Kang X W. Self-supported Ru-Cu_3P catalyst towards alkaline hydrogen evolution. *J. Electrochem.*, 2022, 28(10): 2214005.

Received: 2022-06-23, Revised: 2022-07-26. #These authors contribute equally to the paper. *Corresponding author: Tel: (86-20) 39380520, E-mail: esxkang@scut.edu.cn

sition metal compounds, such as hydroxides, sulfides, selenides, and phosphides[10]. Transition metal phosphides are considered as doping phosphor atoms into the lattice of transition metals[11], where the phosphor atoms behave as H adsorption sites[12]. The phosphor atoms can also withdraw electrons from the metals[13], enhance the adsorption of water molecules on the metal atoms and promote the water splitting in alkaline solution. In an acidic electrolyte, phosphor can facilitate the HER process by enhancing the adsorption of positively charged protons on phosphor atoms[14].

Among the transition metal phosphides[15], copper phosphide (Cu_3P) is considered as an ideal material for development of low-cost and highly active HER catalyst, and its catalytic activity is strongly dependent on the morphology and electronic structures[16]. For example, Jiang and colleagues[17] prepared porous nanosheets of N, P co-doped carbon wrapped Cu_3P, which shows high catalytic activity and long-term stability of HER both in KOH and H_2SO_4 solutions. Sun et al.[18] synthesized the self-supported Cu_3P nanowire arrays by low temperature phosphorization reaction, which needs an overpotential of 143 mV (vs. RHE) to achieve a catalytic current density of 10 $mA\cdot cm^{-2}$.

The alkaline HER activity of the most reported Cu_3P catalysts is still limited by the water dissociation step. It has been widely reported that transition metals with empty d-orbitals can promote the catalytic water splitting on the metallic catalysts[19]. However, this remains unexplored for transition metal phosphides[20], especially for Cu_3P[21]. Ruthenium (Ru) has been demonstrated as an excellent catalyst toward water splitting step due to its emptier *d*-orbitals[22]. In addition, ruthenium phosphides exhibit excellent HER performance in both alkaline and acidic electrolytes, that is comparable to commercial Pt/C[23]. It is anticipated that the doping trace amount of Ru into Cu_3P may remarkably enhance the HER of transition metal phosphides.

Herein, the self-supported Ru-doped Cu_3P catalysts were prepared on copper foam (Ru-Cu_3P/CF), where the water splitting process was accelerated by Ru-doping, due to the electron-deficient d orbitals of Ru, indicating that this strategy is conductive transition metal phosphides and beyond.

2 Experimental Section

2.1 Materials

All reagents were used as received without further purification. Ruthenium trichloride ($RuCl_3$, 99%), potassium hydroxide (KOH, 95%), absolute ethanol (C_2H_5OH, 99%), sodium hydroxide (NaOH, 97%), sodium hypophosphite (NaH_2PO_2, 98%), ammonium persulphate ($(NH_4)_2S_2O_8$, 98%), and hydrochloric acid (HCl, 37%) were purchased from Energy Chemical Co. Copper foam (10 cm × 10 cm) was purchased from Suzhou Kesheng and Metal Materials Company Limited. Deionized water (DI, 18.2 MΩ·cm) was used in all experiments.

2.2 Preparations of Ru-Cu_3P/CF and Contrastive Samples

2.2.1 Synthesis of Ru-Cu_3P/CF

Typically, copper foam (CF) was firstly cleaned by sonication sequentially in hydrochloric acid (1 $mol\cdot L^{-1}$ HCl) and water several times to remove the surface impurities or oxides. The cleaned CF (1 cm × 1 cm) was instantly immersed into a 10 mL aqueous solution containing 1 mmol $RuCl_3$ at room temperature for 2 min to obtain Ru-CF. 0.3 g NaH_2PO_2 and Ru-CF were put at two adjacent porcelain boats, at the upstream and downstream of tube furnace, respectively. The molar ratio of P to Cu was 6:1. Subsequently, the temperature of the tube furnace was elevated to 350 ℃ with a heating rate of 2 $℃\cdot min^{-1}$ under Ar atmosphere and held at this temperature for 120 min. After cooling to room temperature, the obtained sample is denoted as Ru-Cu_3P-1/CF and shows a dark brown color (Figure S1).

Alternatively, fifteen millimoles of $(NH_4)_2S_2O_8$ (3.4 g), 0.25 mol of NaOH (10.0 g), and 100 mL of water were mixed into a 250 mL beaker[24]. Then, a Ru-CF treated sample was placed into the mixed solution at ambient temperature for 40 min to obtain Ru-$Cu(OH)_2$/CF. By following the same phosphorization procedure mentioned above, the obtained sample is named Ru-Cu_3P-2/CF. In addition, Ru-Cu_3P/CF cat

alyst also was prepared by growing $Cu(OH)_2$ on clean CF first, soaked in $RuCl_3$ for 2 min and then phosphorated. The derived sample is denoted as Ru-Cu_3P-3/CF.

Contrastive sample without Ru-doping was prepared by following the same procedure, directly phosphorating $Cu(OH)_2$/CF without soaking in $RuCl_3$ solution. The obtained sample is named Cu_3P/CF.

2.3 Characterizations

Powder X-ray diffraction (XRD, Bruker D8 Advanced, German) test was performed using a Cu K_α radiation source. X-ray photoelectron spectroscopic (XPS) measurements were performed on a PHI X-tool X-ray photoelectron spectrometer using Al as the exciting source. Scanning electron microscopic (SEM) images were recorded by using a Zeiss Supra 55. The hydrogen generation was evaluated by gas chromatography (GC) (HuaAi GC-9560).

2.4 Electrochemical Tests

All the electrochemical experiments were performed with a CHI 660E electrochemical analyzer in a typical three-electrode setup. Ru-Cu_3P/CF or contrastive sample served as the working electrode, whilst a graphite rod and a Hg/HgO served as the counter electrode and reference electrode, respectively.

The electrocatalytic activity toward alkaline HER was studied in 1.0 mol·L^{-1} KOH (pH = 14) solution by linear scanning voltammetry (LSV) with a scanning range of 0.2 to -0.8 V vs. RHE and a sweeping speed of 5 mV·s^{-1}. The durability was evaluated by chronoamperometric profiles at a constant current density. The double-layer capacitance (C_{dl}) values were determined by cyclic voltammetry (CV) at different scanning rates. Electrochemical impedance spectroscopic (EIS) measurements were carried out at frequencies ranging from 100 kHz to 0.01 Hz in a potentiostatic mode. All electrochemical measurements were performed at room temperature (25 ℃) in 1.0 mol·L^{-1} KOH aqueous solution, and the current density was normalized by the geometric area of the electrode.

The electrocatalytic performance of commercial Pt/C was obtained by the following procedure. Two milligrams of commercial Pt/C powder were added to a mixture of 400 mL water and ethanol (V:V = 1:1), followed by 40 μL of 5wt% Nafion solution and sonicated for 30 min to make a 5 mg·L^{-1} catalyst ink. Then, the 12-μL ink was dropped on the cleaned CF, and the resulting sample is recorded as Pt/CF.

3 Results and Discussion

The impacts of the $Cu(OH)_2$ growth and Ru deposition were explored. The Cu_3P/CF catalyst was obtained by directly phosphorating $Cu(OH)_2$/CF without deposition of Ru. The Ru-Cu_3P-1/CF catalyst was prepared by soaking CF directly in $RuCl_3$ solution for galvanic exchange reaction and followed by phosphorization without the procedure of growing $Cu(OH)_2$ nanowires precursor. To prepare the Ru-Cu_3P-2/CF catalyst, CF was soaked in $RuCl_3$ solution for Ru deposition, then followed by growth of $Cu(OH)_2$ nanoarrays and phosphorization.

The $Cu(OH)_2$/CF and Ru-$Cu(OH)_2$/CF precursors were firstly explored by XRD, as shown in Figure 2a. The $Cu(OH)_2$/CF was prepared by growth of $Cu(OH)_2$ on clean Cu foam directly, while the Ru-$Cu(OH)_2$/CF was obtained by doping Ru onto Cu foam surface via galvanic exchange reaction followed by growing $Cu(OH)_2$ nanowires on it. It was observed that XRD peak intensity of $Cu(OH)_2$ (PDF#13-0420) in Ru-$Cu(OH)_2$/CF was much weaker than that of $Cu(OH)_2$/CF. This indicates that the doping of Ru in CF may impede the growth of $Cu(OH)_2$ nanowires on CF.

Thus, the introduction of Ru was finished after the growth of $Cu(OH)_2$ nanowires on CF to obtain

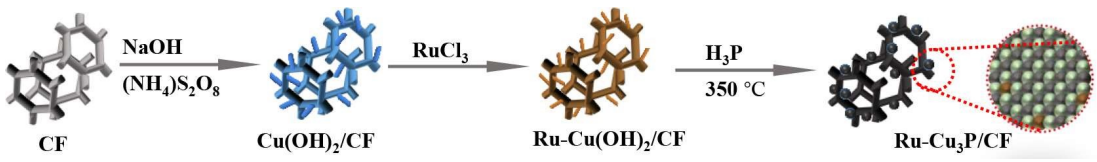

Figure 1 Synthetic scheme of Ru-Cu_3P/CF on copper foam. (color on line)

Ru-Cu_3P-3/CF. After phosphorization, the diffraction peaks for $Cu(OH)_2$ disappeared and the characteristic reflections for the (112), (300) and (113) planes of Cu_3P (PDF#2-1263) at 36.2°, 45.1° and 46.5° emerged[25]. It should be noted that the diffraction pattern of Cu was not observed for both Cu_3P/CF and Ru-Cu_3P-3/CF, which shares the direct growth of $Cu(OH)_2$ nanoarrays on CF, and results in the high coverage of Cu_3P on Cu foam[15]. Since the loading of Ru was quite low, no characteristic peak of ruthenium phosphide was observed in Figure 2b.

The surface states and compositions of Ru-Cu_3P/CF were studied by XPS. Figure 3a displays the fine XPS

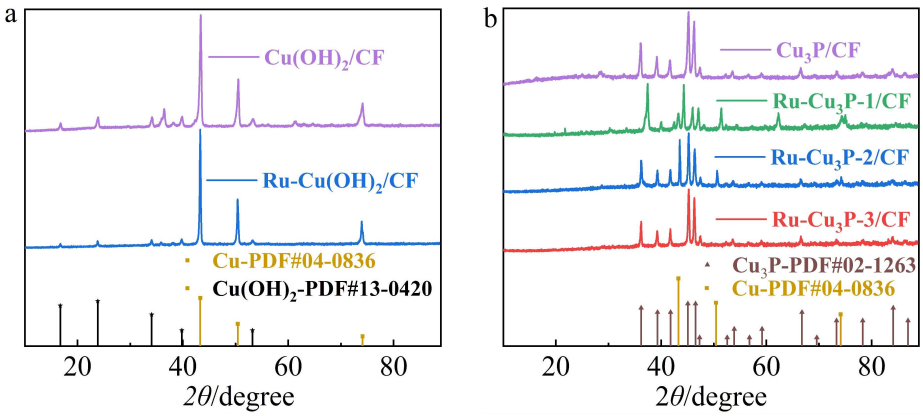

Figure 2 XRD patterns of (a) $Cu(OH)_2$/CF and Ru-$Cu(OH)_2$/CF, and (b) Ru-Cu_3P-1/CF, Ru-Cu_3P-2/CF, Ru-Cu_3P-3/CF and Cu_3P/CF. (color on line)

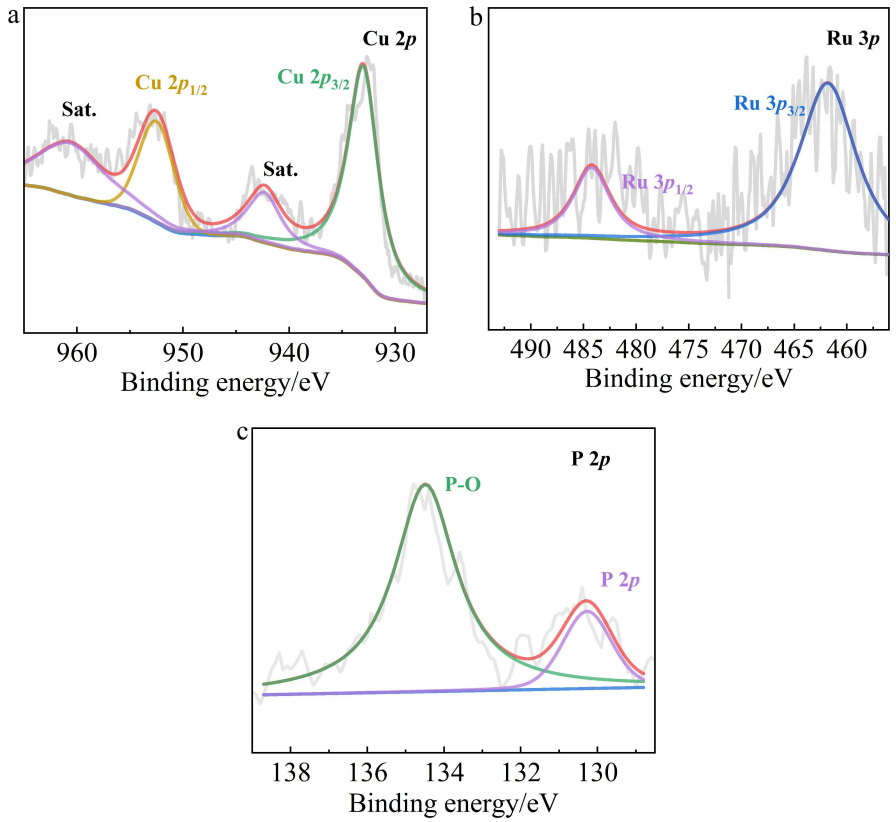

Figure 3 XPS profiles of (a) Cu 2*p*, (b) Ru 3p, and (c) P 2*p* for Ru-Cu_3P-3/CF. (color on line)

spectrum of Cu 2*p* for Ru-Cu_3P-3/CF, where the peaks at 932.9 and 952.4 eV are indexed to the Cu^{1+} $2p_{3/2}$ and $2p_{1/2}$, respectively, in Cu_3P[16], while the peaks at 943.7 and 960.9 eV belong to the satellites of Cu^{1+}. The high resolution XPS spectrum of Ru 3p is shown in Figure 3b, and the two peaks were observed at 484.3 and 461.9 eV[26], which are assigned to Ru $3p_{1/2}$ and $3p_{3/2}$ of RuP_2, respectively[27]. Figure 3c shows the high resolution XPS spectrum of P 2*p* for Ru-Cu_3P-3/CF, where the peak at 134.3 eV was ascribed to P-O due to the surface oxidation upon exposure to atmosphere[28]. The peaks at 130.3 eV was ascribed to P 2*p* of metal phosphide[29]. All the XPS results confirmed the formation of Ru-doped Cu_3P[30].

The surface morphologies of the precursor and CF-supported Ru-Cu_3P/CF were examined by SEM. As shown in Figure S2a-b, the smooth nanowires grew on the copper foam with a diameter of 100 ~ 400 nm. The $Cu(OH)_2$ nanoarrays prepared on clean CF aligned very well. However, upon doping Ru onto CF, the Ru-doped $Cu(OH)_2$ nanoarrays showed disordered alignment. Direct phosphorization of $Cu(OH)_2$/CF resulted in Cu_3P/CF, which revealed nanosheets morphology for Cu_3P/CF (Figure 4a). In contrast, Ru-$Cu(OH)_2$/CF led to Ru-Cu_3P-2/CF and Ru-Cu_3P-3/CF, which displays Cu_3P nanoparticles (Figure 4c and 4d), possibly due to the disordered collapse of nanoarrays upon thermal annealing. Ru-Cu_3P-1/CF (Figure 4b) exhibited only textured surface due to the absence of $Cu(OH)_2$ nanoarrays. Ru-Cu_3P-3/CF was obtained by soaking $Cu(OH)_2$/CF in $RuCl_3$ solution and followed by phosphorization, which results in rougher surface, as shown in Figure 4d, and may provide larger surface area. Element mapping images (Figure S2d-g) demonstrate the successful incorporation of Ru and the uniform distribution of each element on the samples, in agreement with the XPS results. The doping level of Ru in Ru-Cu_3P-X/CF was determined to be as low as 0.1atm% by energy dispersive X-ray spectroscopy in SEM measurement.

In Figure 5a-b, Ru-Cu_3P-1/CF, Ru-Cu_3P-2/CF and Ru-Cu_3P-3/CF required overpotentials of 138.0, 99.0 and 95.6 mV, respectively, to achieve a current density of 10 mA·cm^{-2}, which are much better than that of Cu_3P/CF (245 mV). The Tafel slopes of Ru-Cu_3P-1/CF, Ru-Cu_3P-2/CF and Ru-Cu_3P-3/CF were 105.2, 99.8 and 73.6 mV·dec^{-1}, respectively, indicating that the rate determining step (RDS) is the Heyrovsky step[31]. The Tafel slope of Cu_3P/CF was 136.6 mV·dec^{-1}, much higher than that of Ru-Cu_3P-X/CF, denoting that the

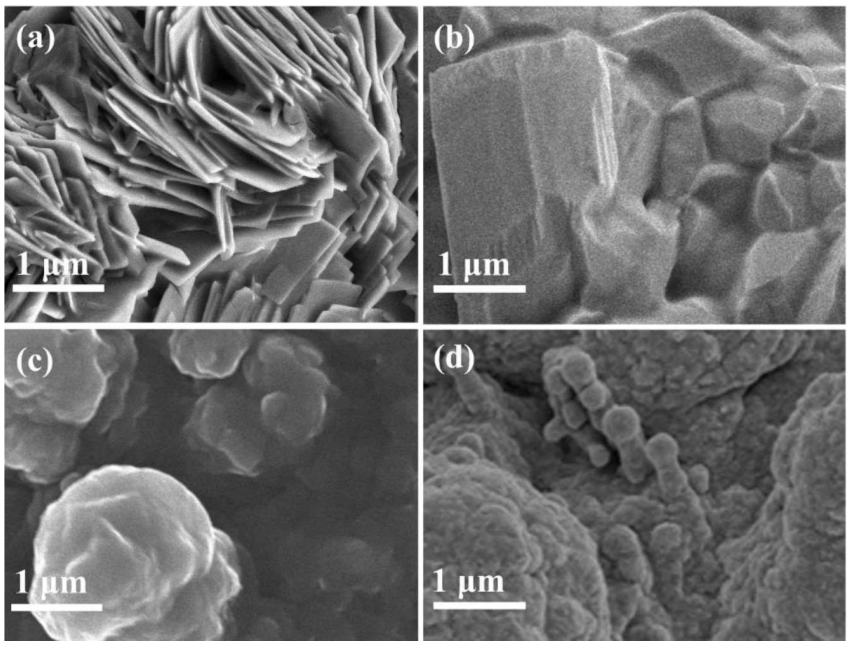

Figure 4 SEM images of (a) Cu_3P/CF, (b) Ru-Cu_3P-1/CF, (c) Ru-Cu_3P-2/CF and (d) Ru-Cu_3P-3/CF.

doping of Ru into Cu_3P can maneuver the RDS from Volmer step on Cu_3P/CF to Heyrovsky step on Ru-Cu_3P-3/CF[32]. The catalytic activity toward alkaline HER for Ru-Cu_3P-3/CF outperformed most of the reported transition metal phosphides in the literatures, as shown in Table S1.

From the semi-circle in the Nyquist plots of EIS measurements[33], the interfacial charge transfer resistance (R_{ct}) can be derived to evaluate the HER kinetics (Figure 5d). Distinctly, the Rct values were in the order of Cu_3P/CF > Ru-Cu_3P-1/CF > Ru-Cu_3P-2/CF > Ru-Cu_3P-3/CF > Pt/CF, which are in agreement with that derived from the LSV measurements. The electrochemical active surface areas (ECSA) of these catalysts were evaluated by the double-layer capacitance at the region of 0.05 ~ 0.35 V (Figure S3)[34]. The capacitance of Ru-Cu_3P-3/CF was 174.74 mF·cm^{-2}, indicating that it has the highest surface roughness and

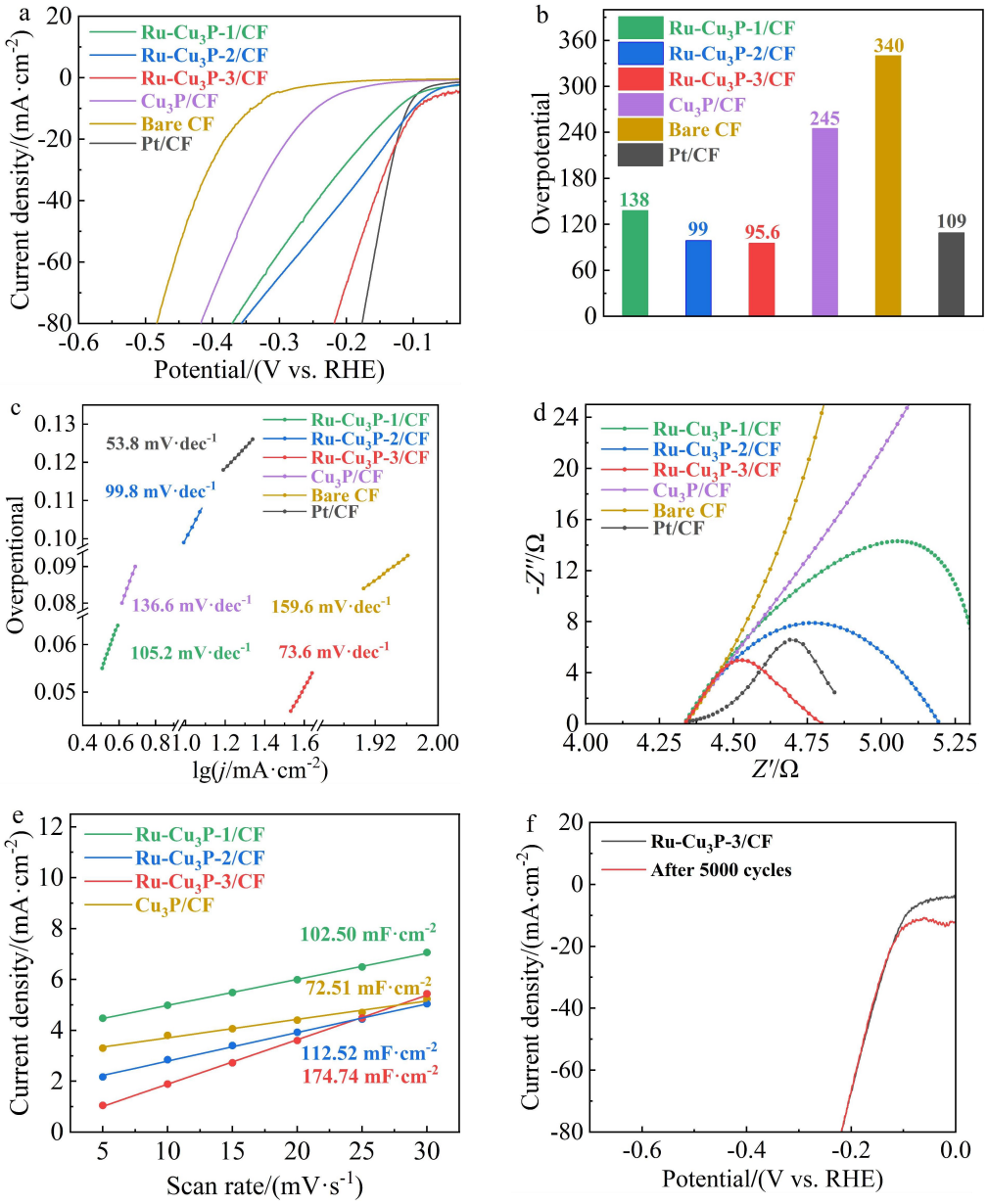

Figure 5 HER performances of Cu_3P/CF, Ru-Cu_3P-X/CF (X = 1, 2, 3) and Pt/C in 1.0 mol·L^{-1} KOH. (a) LSV curves, (b) overpotential plots at 10 mA·cm^{-2}, (c) Tafel plots, (d) Nyquist plots, (e) linear fittings of the capacitive currents for various catalysts at 0.1 V vs. RHE over the potential scan rate and (f) LSV curves on Ru-Cu_3P-3/CF before and after 5000 CV cycles. (color on line)

area (Figure 5e), and could be associated with its larger current density[18]. The ECSA-normalized LSV curves (Figure S4) indicate an over potential of 227 mV at a current density of 0.02 mA cm^{-2} (ECSA), which is lower than those of Ru-Cu_3P-2/CF (268 mV), Ru-Cu_3P-1/CF (283 mV) and Cu_3P/CF (332 mV), suggesting the remarkably higher intrinsic HER activity of Ru-Cu_3P-3/CF t than other catalysts. Figure 5f exhibits an excellent catalytic durability of Ru-Cu_3P-3/CF, after 5000 cycles, the polarization curve of Ru-Cu_3P-3/CF had a negligible shift in the whole potential range. From Figure S5, we could discover that after stability test, the Ru-Cu_3P-3/CF maintained the morphology of the nanoparticles and the elements were evenly distributed on the sample. As shown in Figure S6, the faradaic efficiency of Ru-Cu_3P-3/CF was nearly 100% within 1 h at an overpotential of 95 mV (vs. RHE), indicating an outstanding HER stability.

4 Conclusions

The Ru-Cu_3P/CF catalyst with the porous copper foam substrate and excellent HER performance was synthesized by growth of $Cu(OH)_2$ nanoarrays, doping of Ru and low temperature phosphorization. The results showed that the phosphorization of $Cu(OH)_2$ nanoarrays could significantly increase the electrochemical surface area. The Ru-doping into copper foam could impede the growth of $Cu(OH)_2$ nanoarrays. The Ru-doped Cu_3P catalyst exhibited the remarkably improved HER activity as compared to the pristine Cu_3P, which significantly accelerated the water splitting step, changing the rate determining step from Volmer step to Heyrovsky step. The best-performed Ru-Cu_3P/CF catalyst required an overpotential of 95.6 mV to achieve a current density of 10 mA·cm^{-2} and exhibited a Tafel slope of 73.6 mV·dec^{-1}. The superior alkaline HER catalytic activity of Ru-Cu_3P/CF was also ascribed to the large specific surface area.

Acknowledgements:

This work was supported by the National Natural Science Foundation of China (No. U2032151).

Supporting Information:

Detailed SEM images and CV curves of ECSA measurements.

References:

[1] Zhang L H, Chuai H Y, Liu H, Fan Q, Kuang S Y, Zhang S, Ma X B. Facet dependent oxygen evolution activity of spinel cobalt oxides[J]. J. Electrochem., 2022, 28(2): 139-149.

[2] Huang R Q, Liao W P, Yan M X, Liu S, Li Y M, Kang X W. P-doped Ru-Pt alloy catalyst towards high performance alkaline hydrogen evolution reaction[J]. J. Electrochem., 2022, 27(0): 1-14.

[3] Zheng H Y, Huang X B, Gao H Y, Lu G L, Dong W J, Wang G. Cu@Cu_3P core-shell nanowires attached to nickel foam as high-performance electrocatalysts for the hydrogen evolution reaction[J]. Chem. Eur. J., 2019, 25(4): 1083-1089.

[4] Jin X, Li J, Cui Y T, Liu X Y, Zhang X L, Yao J L, Liu B D. Cu_3P-Ni_2P hybrid hexagonal nanosheet arrays for efficient hydrogen evolution reaction in alkaline solution[J]. Inorg. Chem., 2019, 58(17): 11630-11635.

[5] Wang Z, Du H T, Liu Z, Wang H, Asiri A M, Sun X P. Interface engineering of a CeO_2-Cu_3P nanoarray for efficient alkaline hydrogen evolution[J]. Nanoscale, 2018, 10(5): 2213-2217.

[6] Han A, Zhang H Y, Yuan R H, Ji H X, Du P W. Crystalline copper phosphide nanosheets as an efficient Janus catalyst for overall water splitting[J]. ACS Appl. Mater. Interfaces, 2017, 9(3): 2240-2248.

[7] Swearer D F, Zhao H Q, Zhou L N, Zhang C, Robatjazi H, Martirez J M P, Krauter C M, Yazdi S, McClain M J, Ringe E, Carter E A, Nordlander P, Halas N J. Heterometallic antenna-reactor complexes for photocatalysis[J]. Proc. Natl. Acad. Sci. U.S.A., 2016, 113(32): 8916-8920.

[8] Li W D, Zhao Y X, Liu Y, Sun M Z, Waterhouse G I N, Huang B L, Zhang K, Zhang T R, Lu S Y. Exploiting Ru-induced lattice strain in coru nanoalloys for robust bifunctional hydrogen production[J]. Angew. Chem. Int. Ed., 2021, 60(6): 3290-3298.

[9] Wang Q J, Zhang Z Y, Zhao X Z, Xiao J W, Manoj D, Wei F F, Xiao F, Wang H R, Wang S. MOF-derived copper nitride/phosphide heterostructure coated by multi-doped carbon as electrocatalyst for efficient water splitting and neutral-pH hydrogen evolution reaction[J]. ChemElectroChem, 2020, 7(1): 289-298.

[10] Wei S T, Qi K, Jin Z, Cao J S, Zheng W T, Chen H, Cui X Q. One-step synthesis of a self-supported copper phos-

phide nanobush for overall water splitting[J]. ACS Omega, 2016, 1(6): 1367-1373.

[11] Liu L B, Ge L, Sun Y Y, Jiang B B, Cheng Y F, Xu L, Liao F, Kang Z H, Shao M W. Quasi-layer CO_2P-polarized Cu_3P nanocomposites with enhanced intrinsic interfacial charge transfer for efficient overall water splitting [J]. Nanoscale, 2019, 11(13): 6394-6400.

[12] Kibsgaard J, Tsai C, Chan K, Benck J D, Nörskov J K, Abild-Pedersen F, Jaramillo T F. Designing an improved transition metal phosphide catalyst for hydrogen evolution using experimental and theoretical trends[J]. Energy Environ. Sci., 2015, 8(10): 3022-3029.

[13] Pawar S M, Pawar B S, Hou B, Kim J, Ahmed A T A, Chavan H S, Jo Y, Cho S, Inamdar A I, Gunjakar J L, Kim H, Cha S, Im H. Self-assembled two-dimensional copper oxide nanosheet bundles as an efficient oxygen evolution reaction (OER) electrocatalyst for water splitting applications[J]. J. Mater. Chem. A, 2017, 5(25): 12747-12751.

[14] Li Y, Luo Z Y, Ge J J, Liu C P, Xing W. Research progress in hydrogen evolution low noble/non-precious metal catalysts of water electrolysis[J]. J. Electrochem., 2018, 24 (6): 572-588.

[15] Xu F, Lu J, Luo L L, Yu C, Tang Z, Abbo H S, Titinchi S J J, Zhu J L, Shen P K, Yin S B. Cu_2S-Cu_3P nanowire arrays self-supported on copper foam as boosting electrocatalysts for hydrogen evolution[J]. Energy Technol., 2019, 7(4): 1800993.

[16] Xu T Y, Wei S T, Zhang X L, Zhang D T, Xu Y C, Cui X Q. Sulfur-doped Cu_3P|S electrocatalyst for hydrogen evolution reaction[J]. Mater. Res. Express., 2019, 6(7): 075501.

[17] Jiang E J, Jiang J H, Huang G, Pan Z Y, Chen X Y, Wang G F, Ma S J, Zhu J L, Shen P K. Porous nanosheets of Cu_3P@N,P Co-doped carbon hosted on copper foam as an efficient and ultrastable pH-universal hydrogen evolution electrocatalyst[J]. Sustain. Energy Fuels, 2021, 5(9): 2451-2457.

[18] Tian J Q, Liu Q, Cheng N Y, Asiri A M, Sun X P. Self-supported Cu_3P nanowire arrays as an integrated high-performance three-dimensional cathode for generating hydrogen from water[J]. Angew. Chem. Int. Ed., 2014, 53(36): 9577-9581.

[19] Luo M, Cai J Y, Zou J S, Jiang Z, Wang G M, Kang X W. Promoted alkaline hydrogen evolution by an N-doped Pt-Ru single atom alloy[J]. J. Mater. Chem. A, 2021, 9(26): 14941-14947.

[20] Wang P T, Zhang X, Zhang J, Wan S, Guo S J, Lu G, Yao J L, Huang X Q. Precise tuning in platinum-nickel/nickel sulfide interface nanowires for synergistic hydrogen evolution catalysis[J]. Nat. Commun., 2017, 8: 14580.

[21] Xie Y F, Cai J Y, Wu Y S, Zang Y P, Zheng X S, Ye J, Cui P X, Niu S W, Liu Y, Zhu J F, Liu X J, Wang G M, Qian Y T. Boosting water dissociation kinetics on Pt-Ni nanowires by N-induced orbital tuning[J]. Adv. Mater., 2019, 31(16): 1807780.

[22] Mao J J, He C T, Pei J J, Chen W X, He D S, He Y Q, Zhuang Z B, Chen C, Peng Q, Wang D S, Li Y D. Accelerating water dissociation kinetics by isolating cobalt atoms into ruthenium lattice[J]. Nat. Commun., 2018, 9: 4958.

[23] Chang Q B, Ma J W, Zhu Y Z, Li Z, Xu D Y, Duan X Z, Peng W C, Li Y, Zhang G L, Zhang F B, Fan X B. Controllable synthesis of ruthenium phosphides (RuP and RuP_2) for pH-universal hydrogen evolution reaction[J]. ACS Sustain. Chem. Eng., 2018, 6(5): 6388-6394.

[24] Yao M Q, Wang B J, Sun B L, Luo L F, Chen Y J, Wang J W, Wang N, Komarneni S, Niu X B, Hu W C. Rational design of self-supported Cu@WC core-shell mesoporous nanowires for pH-universal hydrogen evolution reaction [J]. Appl. Catal. B, 2021, 280: 119451.

[25] Dai D M, Wei B, Li Y, Ma X, Liang S, Wang S, Xu L L. Self-supported hierarchical $Fe(PO_3)_2$@Cu_3P nanotube arrays for efficient hydrogen evolution in alkaline media[J]. J. Alloys Compd., 2020, 820: 153185.

[26] Li Y P, Zhang J H, Liu Y, Qian Q Z, Li Z Y, Zhu Y, Zhang G Q. Partially exposed RuP_2 surface in hybrid structure endows its bifunctionality for hydrazine oxidation and hydrogen evolution catalysis[J]. Sci. Adv., 2020, 6(44): eabb4197.

[27] Pu Z H, Amiinu I S, Kou Z K, Li W Q, Mu S C. RuP_2-basedcatalysts with platinum-like activity and higher durability for the hydrogen evolution reaction at all pH values [J]. Angew. Chem. Int. Ed, 2017, 56(38): 11559-11564.

[28] Yu L P, Zhang J, Dang Y L, He J K, Tobin Z, Kerns P, Dou Y H, Jiang Y, He Y H, Suib S L. *In situ* growth of Ni_2P-Cu_3P bimetallic phosphide with bicontinuous structure on self-supported NiCuC substrate as an efficient hydrogen evolution reaction electrocatalyst[J]. ACS Catal., 2019, 9(8): 6919-6928.

[29] Ma X X, Chang Y Q, Zhang Z, Tang J L. Forest-like NiCoP@Cu_3P supported on copper foam as bifunctional electrocatalyst for hydrogen and oxygen evolution reactions[J]. J. Mater. Chem. A, 2017, 6: 2100-2106 .

[30] Wang H, Zhou T T, Li P L, Cao Z, Xi W, Zhao Y F, Ding Y. Self-supported hierarchical nanostructured NiFe-LDH and Cu_3P weaving mesh electrodes for efficient water splitting[J]. ACS Sustain. Chem. Eng., 2017, 6(1): 380-

388.

[31] Hai X, Xi S B, Mitchell S, Harrath K, Xu H M, Akl D F, Kong D B, Li J, Li Z J, Sun T, Yang H M, Cui Y G, Su C L, Zhao X X, Li J, Pérez-Ramírez J, Lu J. Scalable two-step annealing method for preparing ultra-high-density single-atom catalyst libraries[J]. Nat. Nanotechnol., 2022, 17(2): 174-181.

[32] Chen Z, Kronawitter C X, Koel B E. Facet-dependent activity and stability of Co_3O_4 nanocrystals towards the oxygen evolution reaction[J]. Phys. Chem. Chem. Phys., 2015, 17(43): 29387-29393.

[33] Wan R D, Luo M, Wen J B, Liu S L, Kang X W, Tian Y. Pt-Co single atom alloy catalysts: Accelerated water dissociation and hydrogen evolution by strain regulation[J]. J. Energy Chem., 2022, 69: 44-53.

[34] Wei Z Q, Hu X, Ning S L, Kang X W, Chen S W. Supported heterostructured MoC/Mo_2C nanoribbons and nanoflowers as highly active electrocatalysts for hydrogen evolution reaction[J]. ACS Sustain. Chem. Eng., 2019, 7(9): 8458-8465.

泡沫铜支撑 Ru 掺杂 Cu_3P 自支撑催化剂及其析氢性能

万紫轩#,王超辉#,康雄武*

(华南理工大学环境与能源学院新能源研究所, 广东 广州 510006)

摘要: 过渡金属磷化物(TMP)是一种用于碱性条件下析氢反应(HER)的有效催化剂, 然而其活性严重受限于水解离步。本文通过在泡沫铜(CF)上生长 $Cu(OH)_2$ 纳米阵列, $RuCl_3$ 溶液浸泡和磷酸化, 制备了一种具有较大比表面积和适当 Ru 掺杂的 Ru-Cu_3P 自支撑催化剂 (Ru-Cu_3P/CF)。作为一种优良的 HER 催化剂, 在电流密度为 10 mA·cm^{-2} 时, 其过电位为 95.6 mV, 比 Cu_3P/CF 降低 149.4 mV。其决速步由 Volmer 向 Heyrovsky 机制过渡。HER 性能的提高可以归因于 Ru 掺杂磷化铜促进水解离过程,以及 $Cu(OH)_2$ 纳米阵列衍生 Cu_3P 纳米结构具有更高的电化学活性面积, 从而保证了更多的活性位点。本论文突出了具有空的 *d* 轨道的金属掺杂促进水解离的重要性, 为高性能电解水析氢催化剂的设计提供了新思路。

关键词: 电催化;水解离;析氢反应;磷化亚铜;钌掺杂